JOC The Journal of Organic Chemistry

Featured Article

pubs.acs.org/joc

Synthesis, Theoretical Analysis, and Experimental pK_a Determination of a Fluorescent, Nonsymmetric, In−Out Proton Sponge

Lee Belding, Peter Stoyanov, and Travis Dudding*

Brock University, 500 Glenridge Avenue, St. Catharines, ON L2S 3A1, Canada

Supporting Information

ABSTRACT: Herein, we report the synthesis and theoretical investigation of a nonsymmetric bis(diisopropylamino)cyclopropenimine (DAC)-functionalized proton sponge derivative, coined the "Janus" sponge. The reported sponge was isolated as a monoprotonated salt, though no intramolecular hydrogen bond was observed. Homodesmotic equations supported the absence of a N−HN intramolecular hydrogen bond and a relatively low freebase strain, while DFT calculations and X-ray crystallography revealed the presence of a hydrogen bond to the Cl^- counterion. Associated with this fact was the rare in−out geometry of the basic nitrogens, which represents the first such instance in a proton sponge not having an *ortho*-substituent and/or being in a protonated state. Furthermore, N_{LP} donation into the cyclopropenium cation was found to stabilize this unprecedented in−out geometry. The measured pK_a was determined to be 23.8, in good agreement with the computed value of 23.9. Lastly, the Janus sponge was found to have fluorescent properties both in the solid state and in solution, which notably represents the first example of a cyclopropenimine-based fluorescent organic compound.

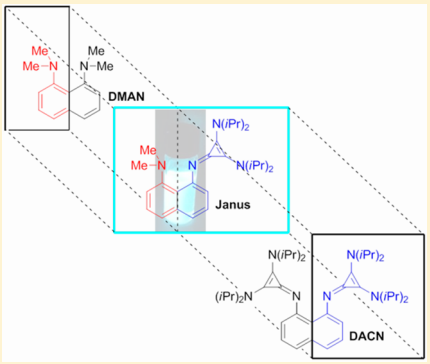

INTRODUCTION

The interplay between molecular strain, intramolecular hydrogen bond (IHB) energy, and basicity in proton sponges has led to many scientific insights, which have undoubtedly influenced our fundamental understanding of chemistry, far beyond just the prototypical proton sponge.[1] In particular, the study of hydrogen bonding (H-bonding) within proton sponges has provided rigorous knowledge into the inter-related roles of symmetry, resonance, and aromaticity in H-bonding, as well as a better understanding of kinetic versus thermodynamic basicity and the emergence of a more refined view of the entropic and enthalpic factors contributing to H-bond strength.[2] Of biological relevance, the knowledge gained from proton sponges has provided further insight into amide N- versus O-protonation states and the mechanism of acid-catalyzed amide hydrolysis in peptides, in addition to fostering a more informed understanding of the importance of short and strong hydrogen bonding in various enzymatic processes.[3] Meanwhile, overshadowing these developments, at least from a fundamental stance, has been the influential impact they have had on current theories surrounding proton transfer rates,[4] charge transfer states,[5] and unusual hydrogen bonding.[6]

Much like the proton sponge **1**, the bis(dialkylamino)-cyclopropenimine (DAC) motif began as nothing more than a theoretical curiosity,[7] a simple extension of the cyclopropyl cation.[8] However, over time, continued study has led to numerous insights into its chemical and electronic properties,[9] and DACs have since found applications in organocatalysis[10] and phase transfer catalysis[11] or, alternatively, use as ionic liquids,[12] polyelectrolytes,[13] components of nitrogen-based ligands,[14] and superbases.[15] In considering the related parallels between proton sponges and DACs, both in terms of origin and demonstrated utility, we recently merged these two molecular entities with the synthesis DACN (**2**)[16] and its diprotonated analogue, DACN·2H$^+$ (**2**·2H$^+$) (Figure 1). Not unexpectedly, **2** was found to be an exceptionally strong, neutral, organic superbase, having a conjugate acid with a computed pK_a value of 27.0 and a proton affinity (PA) of 282.3, yet unfortunately to date, only the freebase and its diprotonated salt have been isolated, which has hampered efforts to obtain an experimentally derived pK_a measurement of **2**.[16]

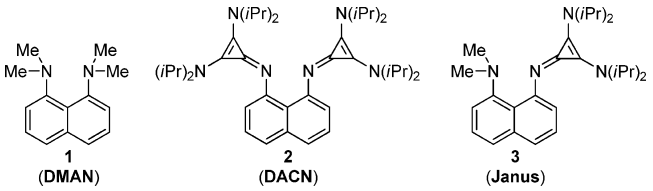

Figure 1. Structures of the proton sponges DMAN (**1**), DACN (**2**), and Janus sponge (**3**).

Given this obstacle and a focus on cultivating a comprehensive understanding of hydrogen bonding in DACs as a means to facilitate a longer-term agenda of rationally designing new catalysts, ligands, and materials, we set out to synthesize a nonsymmetric DAC-susbtituted proton sponge

Received: August 4, 2015
Published: October 6, 2015

DOI: 10.1021/acs.joc.5b01743
J. Org. Chem. 2016, 81, 6−13

Scheme 1. Synthesis of the Janus Sponge 3

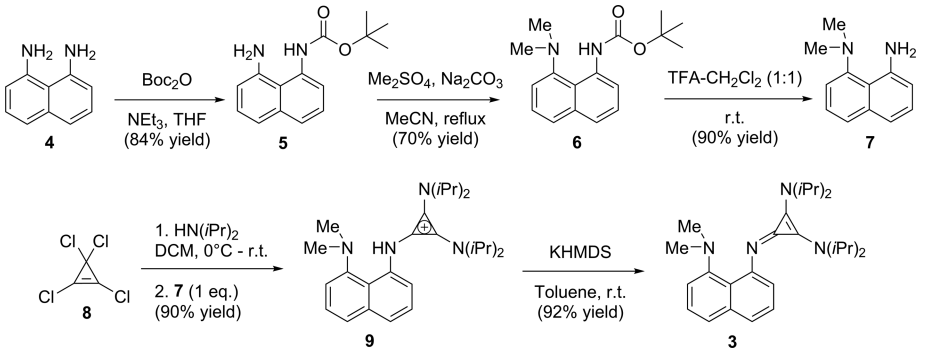

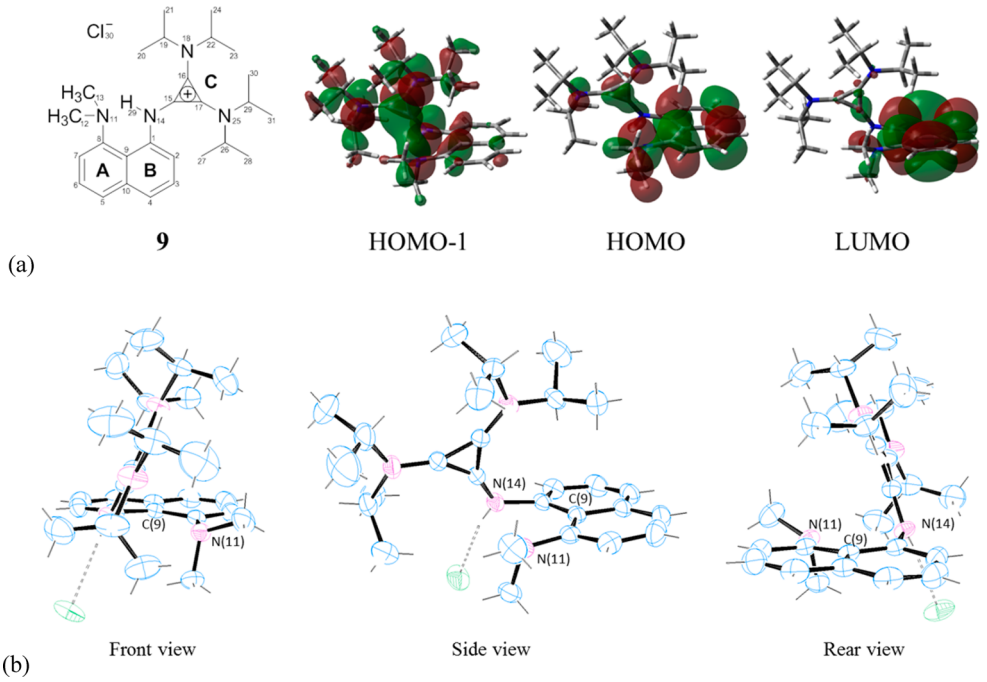

Figure 2. (a) Two-dimensional representation and corresponding numbering scheme for compound **9** and selected B3LYP/6-31G(d,p) computed MOs for $\mathbf{9}_{xray}$. (b) ORTEP3-generated X-ray structure of compound **9** (purple = nitrogen, blue = carbon, green = chlorine). Thermal ellipsoids are displayed at 50% probability.

derivative akin to DACN and Alder's archetypical sponge. Nonsymmetric proton sponges are an under-represented class, despite their considerable potential to foster unique conceptual understanding and open innovative inroads to chemical advancement.[7,17] Not only would this nonsymmetric sponge provide us with information relating to how protonated DACs interact with sp^3 nitrogen centers, but it was envisioned that it might be amenable to isolation as a monoprotonated adduct and allow for an accurate experimental determination of its pK_a. Accordingly, reported herein is the synthesis and theoretical investigation of a nonsymmetric proton sponge derivative having 1,8-napthlyl-substituted $N_{(sp2)}$- and $N_{(sp3)}$-hybridized nitrogens, comprised on the one hand from a prototypical DMAN sponge and on the other the DACN sponge and is thus fittingly coined the "Janus sponge" (**3**).[18] As an added dimension, the synthetic route to **3** also allows for the synthesis of various other nonsymmetric proton sponges having unique properties. Lastly, this report revisits the internal charge-transfer-based fluorescence associated with **1**, in the context of a nonsymmetric variant.

RESULTS AND DISCUSSION

The synthesis of **3** began from commercially available 1,8-diaminonaphthalene, which was selectively monoprotected using the procedure of MacLachlan et al.,[19] followed by methylation of the free nitrogen with dimethyl sulfate. TFA-mediated *N*-Boc deprotection then afforded **7** in 53% yield (Scheme 1). The dialkylaminocyclopropenyl group was then installed by sequential dropwise addition of diisopropylamine to a DCM solution of tetrachlorocyclopropene (**8**) at 0 °C, followed by a solution of **7** in DCM, and the resulting reaction mixture was stirred for 6 h to provide salt **9** in 90% yield after workup. In turn, the freebase **3** was obtained in 92% yield (44% overall yield for five steps) using 0.5 M KHMDS in toluene or alternatively NaH in THF. Unlike its counterpart DACN (**2**), the nonsymmetrical sponge **9** was not susceptible to diprotonation in the presence of moderately strong acids, such as acetic acid or concentrated HCl. The observed inability of **9** to undergo a second protonation likely stems from an increase in strain that would arise from introducing a second proton.

DOI: 10.1021/acs.joc.5b01743
J. Org. Chem. 2016, 81, 6−13

X-ray quality crystals of the hydrochloride salt ($\mathbf{9}_{xray}$) were then obtained by vapor diffusion crystallization from benzene/EtOAc (see Experimental section for details), and the corresponding molecular structure was determined by single-crystal X-ray diffraction analysis (Figure 2). The structure of $\mathbf{9}_{xray}$ was immediately striking for several reasons. First, in keeping with previously reported $\mathbf{2}\cdot 2H^+$,[16] the typical N(11)···H(29)−N(14) IHB observed in most proton sponges is absent, having been superseded by a N(14)H(29)···Cl(30) hydrogen bond to the chloride counterion (2.29 Å). Furthermore, the relatively long N(11)···N(14) interatomic distance (2.81 Å) and noticeable distortion of the naphthalene backbone ($\theta_{5-10-9-1}$ = 175.4°) were more consistent with that of a neutral proton sponge.[5] Another distinguishing feature was the hybridization of N(14), which according to natural bond order (NBO) analysis, displayed significant sp^3 character and the presence of a lone pair. This feature is particularly intriguing as the orientation of the lone pair implied that the two amino groups adopted an in−out configuration (Figure 3), where the

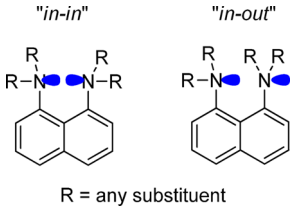

Figure 3. Two-dimensional depiction of the in−in (left) and in−out (right) lone pair configurations in proton sponges.

N(11) electron pair is pointed in toward N(14), but the electron pair of N(14) directed outward from the naphthalene ring. Though this type of geometry is not without precedence,[20] to the best of our knowledge, it represents the first reported isolation of a proton sponge with an in−out configuration lacking an *ortho*-substituent and the first instance of this type of configuration in a protonated proton sponge. In addition to this surprising in−out configuration, the cyclopropenimine ring (ring C) was oriented overtop of the naphthalene backbone (ring A/B), opposite to what has been observed in previously reported proton sponges having basic sp^2 nitrogens, including DAC-substituted sponge **2**.[18,21] While all of the factors responsible for this unprecedented geometry are uncertain, one contributing element leading to this unusual geometry is a stabilizing donor−acceptor interaction between the N(11) lone pair and the cyclopropenyl π-system (N(11)···C(15) = 2.84 Å), as revealed by NBO analysis ($N(11)_{LP} \rightarrow C(15)_{\sigma^*}$, E_{NBO} = 3.1 kcal/mol), and the computed MOs of $\mathbf{9}_{xray}$ (Figure 2, HOMO−1).

In contrast to the X-ray crystal structure, the DFT B3LYP/6-31G(d,p) optimized geometry of **9** ($\mathbf{9}_{opt}$), lacking a chloride ion, did possess a N(11)···H(29)−N(14) intramolecular hydrogen bond (1.77 Å), though the geometry obtained when optimized in the presence of the Cl^- counterion matched the crystal structure quite closely, leading us to believe that the observed molecular geometry of $\mathbf{9}_{xray}$ is not simply an effect of crystal packing forces.

A detailed inspection of computed $\mathbf{9}_{opt}$ proved instructive as the aromatic naphthalene backbone ($\theta_{5-10-9-1}$ = 178.3°) was found to be less distorted and the N(11)···N(14) interatomic distance of 2.68 Å was significantly shorter than that in $\mathbf{9}_{xray}$, due to the presence of a highly nonsymmetric IHB having a N(14)−H(29) bond distance of 1.05 Å and N(11)···H(29) H-bonding contact measuring 1.77 Å. Furthermore, the in−in electron pair configuration in $\mathbf{9}_{opt}$ (Figure 3) allowed for the effective delocalization of the N(14) lone pair into the naphthalene ring system, resulting in ring C being tilted away from the naphthalene backbone and providing a geometry that was more in line with that of conventional proton sponges. Interestingly, the computed geometry of freebase **3** ($\mathbf{3}_{opt}$) shown in Figure 4 closely resembled that of $\mathbf{9}_{xray}$, more so than $\mathbf{9}_{opt}$. Manifesting from the N(11), N(14) lone pair−lone pair repulsion in $\mathbf{3}_{opt}$ was a substantial distortion of the naphthalene backbone from ideal planarity ($\theta_{5-10-9-1}$ = 171.4°) concomitant with elongation of the N(11)···N(14) interatomic distance to 2.91 Å. Meanwhile, the calculated N(14)−C(1) bond distance of 1.40 Å was slightly shorter than the N(11)−C(8) bond distance (1.42 Å) yet longer than the N(14)−C(15) bond distance (1.32 Å). Like $\mathbf{9}_{xray}$, $\mathbf{3}_{opt}$ displayed an in−out-type geometry with ring C tilted toward the A/B ring system, and as such, it would appear that the Janus sponge, regardless whether or not it is protonated, favors an in−out lone pair−lone pair geometry with the cyclopropenyl ring geared inward toward the naphthalene ring. Thus, it would clearly seem that the observed molecular structure of **9** was not simply a result of a strong N(14)H(29)···Cl(30) hydrogen bond to the chloride ion but instead originates from the aforementioned stabilizing donor−acceptor interaction between the N(11) lone pair and the cyclopropenyl π-system.

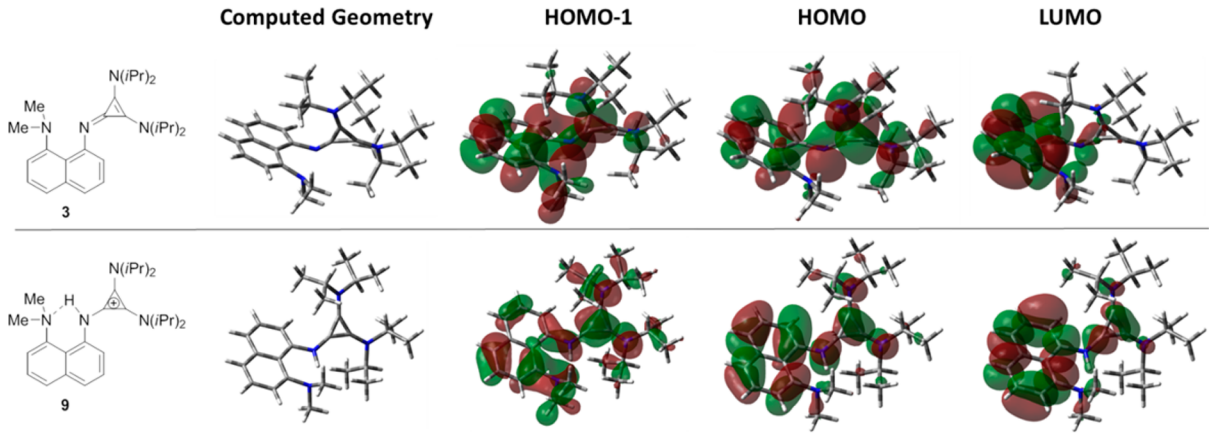

Figure 4. B3LYP/6-31G(d,p) optimized geometries and selected MOs for compounds $\mathbf{3}_{opt}$ and $\mathbf{9}_{opt}$.

DOI: 10.1021/acs.joc.5b01743
J. Org. Chem. 2016, 81, 6−13

Shown in Figure 4 are the corresponding HOMO−1, HOMO, and LUMO of $\mathbf{3}_{opt}$ and $\mathbf{9}_{opt}$. In both cases, the HOMO possesses significant orbital density on the cyclopropenyl ring, which is consistent with previous reports detailing the electron-rich nature of the cyclopropenyl cation,[22] as well as those reports of further oxidizing the cyclopropenyl cation to the radical dication.[23] In this respect, there was minimal contribution from the N(11) lone pair in the HOMO of $\mathbf{9}_{opt}$ or $\mathbf{3}_{opt}$, as evidenced by the lack of orbital density.

In terms of the HOMO−1, $\mathbf{3}_{opt}$ displays substantial orbital contribution from the N(11) lone pair and the cyclopropenyl ring system, which is perhaps not surprising considering the similar geometry to $\mathbf{9}_{xray}$. Nevertheless, even though $\mathbf{9}_{opt}$ also displayed significant contribution from the N(11) lone pair and cyclopropenyl ring system in the HOMO−1, the lobes are not oriented toward one another nor are they of the same sign, in contrast to $\mathbf{3}_{opt}$. Lastly, both LUMOs are primarily centered on the naphthalene backbone, with only a small contribution from the cyclopropenyl ring system in $\mathbf{9}_{opt}$.

At that stage, to ascertain the respective aromaticity of the A, B, and C ring systems, nucleus-independent chemical shift (NICS) calculations[24] were performed on $\mathbf{3}_{opt}$, $\mathbf{9}_{opt}$, and $\mathbf{9}_{xray}$ at the center of each ring system (NICS(0)), as well as 1 Å above (NICS(1)) and 1 Å below (NICS(−1)) the center of each ring to circumvent σ-contamination from the carbon framework of the ring, which is particularly prominent within the small cyclopropenyl ring systems. As seen from Table 1, there is an increase in the NICS values for all three ring systems upon protonation of N(14), regardless of the geometry. For $\mathbf{9}_{opt}$, the increase in NICS values for rings A and B is consistent with the formation of an IHB, wherein the N(11) lone pair is oriented orthogonal to the naphthalene ring, substantially diminishing perturbation of the aromatic backbone. However, in the case of $\mathbf{9}_{xray}$, there is no IHB, and the increase in aromaticity of the A/B ring system is likely a consequence of N(11) lone pair donation into ring C rather than into ring A. Not surprisingly, an increase in the C ring NICS values occurred for both $\mathbf{9}_{xray}$ and $\mathbf{9}_{opt}$, presumably as a direct result of generating the cyclopropenyl cation upon protonation. The noticeably larger NICS value of ring C in $\mathbf{9}_{xray}$ relative to that in $\mathbf{9}_{opt}$ conceivably originates from the N(11) lone pair donation into the cyclopropenyl cation, thus suggesting that the geometry of $\mathbf{9}_{xray}$ is more conducive to cyclopropenyl cation stabilization.

Table 1. B3LYP/6-311++G(d,p)//B3LYP/6-31G(d,p) Calculated NICS(−1), NICS(0), and NICS(1) Values for 3, $\mathbf{9}_{opt}$, and $\mathbf{9}_{xray}$

		$\mathbf{3}_{opt}$	$\mathbf{9}_{opt}$	$\mathbf{9}_{xray}$
ring A	NICS(−1)	9.22	10.80	10.46
	NICS(0)	8.11	9.39	8.76
	NICS(1)	9.43	10.31	10.01
ring B	NICS(−1)	9.28	10.15	9.97
	NICS(0)	8.34	8.76	8.97
	NICS(1)	10.13	9.57	10.56
ring C	NICS(−1)	8.72	8.78	9.22
	NICS(0)	29.84	31.08	32.20
	NICS(1)	8.46	8.96	9.08

Subsequently, to determine the likelihood of **3** being a strong organic base, presumably a superbase, the PA was computed at the B3LYP/6-311G++(d,p)//B3LYP/6-31G(d) level, taking into account thermal corrections estimated at the B3LYP/6-31G(d) level resulting in a computed gas phase basicity of 266.8 kcal/mol, which for reference was substantially less than that of DACN (282.3 kcal/mol) computed at the same level of theory. A relative pK_a (MeCN) calculation at the IEFPCM/B3LYP/6-311G++(d,p)//B3LYP/6-31G(d,p) level, using 1,8-bis(tetramethylguanidino)naphthalene as a reference base, estimated the pK_a value at 23.9 in MeCN. For comparison, the pK_a of DACN computed at the same level of theory was 27. To substantiate these computational results, the pK_a of **3** was experimentally measured in MeCN using a previously reported NMR titration approach.[10a] Gratifyingly, using 1,1,3,3-tetramethylguanidine as a reference base, the measured pK_a value of 23.8 was very close to the computed value. It is interesting to note the lower pK_a of **3**, relative to *t*-Bu-(bisdiisopropylamino)-cyclopropenimine, as it would appear the withdrawing effect of the naphthalene ring decreases the basicity more than it is increased by the presence of an IHB and ground state destabilization.

With respect to the effects of geometric constraints on basicity, the homodesmotic reactions in Scheme 2 were applied to discern between the effect of ground state stabilization (eq 1) and IHB strength (eq 2) on the basicity of **3**. According to eq 1, ground state stabilization contributes 7.7 kcal/mol, while the stabilization associated with the IHB was found to be only 0.6 kcal/mol. Table 2 provides a useful comparison between **3** and **2** and clearly shows that the roughly 1000 times difference in pK_a originates predominantly from a drastic decrease in the freebase strain. Though the hydrogen bond energy in **3** was only one-half that observed in **2**, its effect on the pK_a is likely not as significant. Subsequently, the nature of this IHB was further probed by NBO and QTAIM analysis. Within the

Scheme 2. Homodesmotic Reaction Scheme for the Determination of H-Bonding Strength and Ground State Destabilization

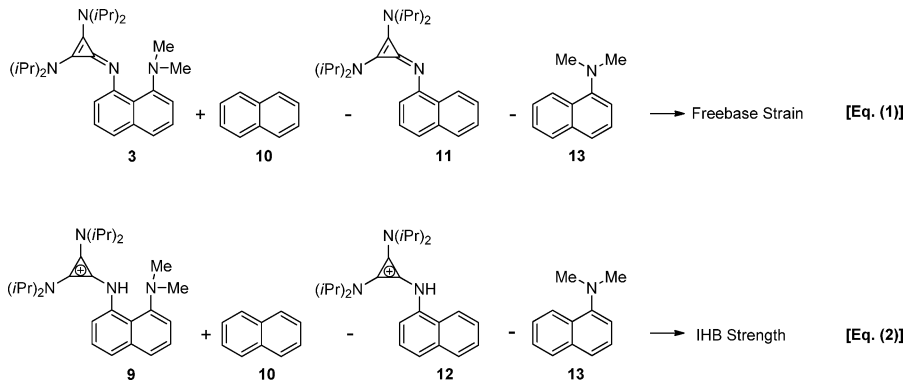

DOI: 10.1021/acs.joc.5b01743
J. Org. Chem. 2016, 81, 6−13

Table 2. Comparison between Janus and DACN

	IHB E_{NBO} (kcal/mol)	IHB strength (eq 2) (kcal/mol)	freebase strain (eq 1) (kcal/mol)	computed PA (kcal/mol)	calcd pK_a	measd pK_a
3 (Janus)	26.0	0.6	7.7	266.8	23.9	23.8
2 (DACN)	27.3	1.2	21.1	282.3	27.0	

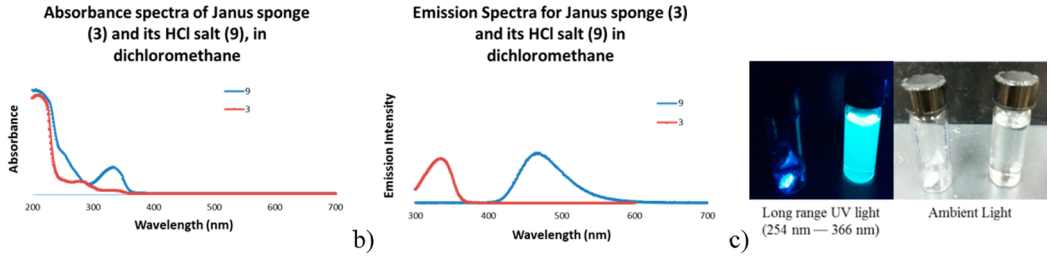

Figure 5. (a) UV/vis absorption spectra of **3** and **9** as 1×10^{-5} M solutions in dichloromethane. (b) Emission spectra of **3** and **9** as 1×10^{-5} M solutions in dichloromethane. Emission spectra taken at room temperature, with entrance and exit slit widths of 5 mm. (c) Visual portrayal of the luminescent character of compound **9** as a solid (left vial) and as a solution in dichloromethane (right vial).

context of QTAIM analysis, the presence of a (3,−1) bond critical point indicative of a maximum of electron density (i.e., a bonding interaction) between the N(11) and H(29) supported the presence of an intramolecular hydrogen bond, and NBO analysis revealed a 23.5 kcal/mol donation of the $N(11)_{LP}$ into the N(14)−H(29) bond. Given the lower ground state destabilization and relatively weak IHB, it is perhaps not surprising that **9** possesses a hydrogen bond to the chloride ion rather than an IHB.

By far, one the most intriguing features of the Janus sponge **3** was its luminescent properties. Upon absorption of UV light ($\lambda_{max} = \lambda_{ex}$ = 283 nm) in a dichloromethane solution at room temperature, **3** emits UV light at a longer wavelength (λ_{em} = 341 nm), corresponding to a Stokes shift of 58 nm (Figure 5). Conversely, a dichloromethane solution of its protonated salt, **9**, absorbs light in the long-range UV region ($\lambda_{max} = \lambda_{ex}$ = 333 nm) and emits light in the visible wavelength (λ_{em} = 472 nm), corresponding to a Stokes shift of 139 nm (Figure 5). Interestingly, this trend is opposite to that reported with **1** in acetonitrile, wherein the neutral species absorbs at a higher wavelength (λ_{max} = 340 nm) than the protonated species (λ_{max} = 286 nm).[25] The change in Stokes shift and fluorescence intensity between **3** and **9** is substantial, though not all too surprising considering the generation of aromaticity upon protonation, which constitutes a considerable geometric and electronic transformation. Notably, under persistent illumination, **9** fluoresces indefinitely as a solid and in solution (Figure 5c), having a quantum yield of 0.37 in ethanol (see Supporting Information for details).

There has been extensive study into the photophysical properties of DMAN, which may shed light on the possible fluorescent origins of **3**.[25,26] According to these reports, the electronic excitation of DMAN originates from its ^1L_a state, with considerable contribution from the NMe_2 groups, and after internal conversion leads to the emissive, naphthalene-based, $1\pi^*$ internal charge transfer state. Twisting of the methyl groups on N(11) (i.e., geometry reorganization) plays a major role in the large Stokes shift. Considering this role of NMe_2 in the fluorescence of DMAN, the NMe_2 group of the Janus sponge is likely important for its luminescent characteristics. Furthermore, there is little doubt that the aromatic cyclopropenium ion also plays a key role in the electronic transition(s) leading to fluorescence, considering that it is the only structural difference from DMAN. From these two conjectures (that the NMe_2 group and cyclopropenium ion are key factors in Janus's luminescent characteristic) and given that the computed LUMO of $\mathbf{9}_{xray}$ (or the LUMO+1 for that matter; see Supporting Information) does not possess significant contribution from either the NMe_2 group or the cyclopropenium ion, excitation likely originates from a MO involving both the cyclopropenyl cation and the NMe_2 group (i.e., the HOMO or HOMO−1), while emitting from a MO involving the naphthalene system.

Though the exact electronic transitions leading to **9**'s fluorescent properties remain uncertain, the drastic effect observed upon adding a single cyclopropenimine unit is evidence that cyclopropenimine-based fluorescent probes, LEDs, and dyes may be worth studying. This robust fluorescent nature of **9** expands the potential applications of cyclopropenimines, especially considering that it represents a fluorescent compound derived from the protonation of a neutral, organic superbase, with the potential to be a bidentate metal chelating ligand.

CONCLUSION

In conclusion, we have reported the synthesis and theoretical investigation of a nonsymmetric, DAC-functionalized proton sponge derivative, coined the "Janus" sponge. The protonated cyclopropenimine unit displayed weak hydrogen bonding to the adjacent NMe_2 substituent and was found to be superseded by a hydrogen-bonding interaction to a Cl^- counterion. Associated with this fact was the rare in−out geometry of the basic nitrogens, which represents the first such instance in the absence of an *ortho*-substituent as well as in a protonated state. Furthermore, N_{LP} donation into the cyclopropenium cation was found to stabilize its unprecedented geometry. The pK_a of **3** was measured to be 23.8, in good agreement with the computed value of 23.9. Lastly, **9** displayed vibrant luminescence both in solution and in the solid phase, representing the first example of a cyclopropenimine-based fluorescent organic compound.

EXPERIMENTAL SECTION

Computational Methodology. Calculations were carried out at the Kohn−Sham hybrid DFT B3LYP[20−22] level of theory using the Gaussian 09[23] and GaussView v5.0.8 programs. To account for solvent effects, the integrated equation formalism polarized continuum solvation model (IEFPCM)[24] was used throughout the computations.

DOI: 10.1021/acs.joc.5b01743
J. Org. Chem. 2016, 81, 6−13

All minima were confirmed by the presence of only real vibrational frequencies. QTAIM calculations were computed using AIM2000.[25]

Materials and Methods. Materials were obtained from commercial suppliers and were used without further purification, unless otherwise specified. All reactions were performed under an inert atmosphere. Reactions were monitored by thin layer chromatography (TLC) using TLC silica gel 60 F254. NMR spectra were obtained with a 300 MHz spectrometer (^{1}H 300 MHz, ^{13}C 75.5 MHz or ^{13}C 150.9 MHz, ^{19}F 292.4 MHz, ^{11}B 96.3 MHz). The chemical shifts are reported as δ values (ppm) relative to tetramethylsilane. FT-IR spectra were obtained with an attenuated total reflectance spectrophotometer from a neat sample. HRMS (high-resolution mass spectrometry) spectra were measured using electrospray ionization (ESI) and a time-of-flight (TOF) mass analyzer in positive ionization mode. Absorption spectra were measured using a UV−vis−NIR spectrophotometer at ambient temperature. Emission spectra were obtained on a xenon flash lamp fluorescence spectrophotometer at ambient temperature with entrance and exit slit widths set to 5 mm.

*tert-Butyl-(8-aminonaphthalen-1-yl)carbamate (**5**).*[19] To a flame-dried 100 mL round-bottom flask backfilled with $N_{2(g)}$ was added 2 g (12.6 mmol, 1 equiv) of 1,8-diaminonaphthalene followed by the addition of 40 mL of dry THF and 2 mL (27.2 mmol, 2.1 equiv) of NEt_3, all via syringe. To the resulting mixture was added dropwise 3 g (13.9 mmol, 1.1 equiv) of di-*tert*-butyldicarbonate dissolved in 10 mL of THF, followed by stirring for 24 h at room temperature. After 24 h, the THF was removed under reduced pressure using a rotary evaporator (153 mbar). The crude product mixture was dissolved in 20 mL of toluene and washed with 10 mL of 1 M NaOH, 10 mL of brine, and then 10 mL of distilled H_2O. The organic layer was subsequently dried over $MgSO_4$, gravity-filtered through a funnel, and the solvent removed under reduced pressure using a rotary evaporator. Purified compound could be acquired by flash chromatography (20% ethyl acetate in hexanes). The final product was isolated as red crystals in 84% yield: ^{1}H NMR (300 MHz, $CDCl_3$) δ = 9.79 (s, 1H), 8.08 (d, J = 7.3 Hz, 1H), 7.49 (t, J = 7.7 Hz, 1H), 7.40 (m, 2H), 7.22 (t, J = 7.7, 1H), 6.78 (d, J = 7.2 Hz, 1H); ^{13}C NMR (75 MHz, $CDCl_3$) δ = 153.3, 140.9, 136.3, 135.5, 126.1, 125.6, 123.6, 122.7, 118.9, 116.9, 116.8, 80.2, 28.5; IR (neat) 3362 cm^{-1}, 3300 cm^{-1} (N−H stretch, primary amine), 3050 cm^{-1} (C−H, aromatic stretch), 2977 cm^{-1} (C−H stretch, alkane), 1687 cm^{-1} (C═O stretch, amide), 1152 cm^{-1} (C−O stretch).

*tert-Butyl-(8-(dimethylamino)naphthalen-1-yl)carbamate (**6**).* To a 100 mL round-bottom flask containing 1 g (3.8 mmol, 1 equiv) of **5** was added 2.1 g (25.1 mmol, 6.5 equiv) of Na_2CO_3. The flask was then fitted with a reflux condenser, backfilled with $N_{2(g)}$, and 50 mL of acetonitrile was added. To the resulting solution was then added 2.6 mL (26.9 mmol, 7.0 equiv) of freshly distilled Me_2SO_4. The reaction mixture was heated to reflux and stirred for 12 h. The mixture was concentrated under reduced pressure, using a rotary evaporator (153 mbar), diluted with 30 mL of H_2O, and extracted three times with 10 mL of dichloromethane. The combined organic extracts were dried over $MgSO_4$, gravity-filtered, and the solvent was removed under reduced pressure. Purified compound could be acquired by flash chromatography (12.5% ethyl acetate in hexanes). The final product was isolated as a clear oil in 70% yield (3.4 mmol, 0.98 g): ^{1}H NMR (300 MHz, $CDCl_3$) δ = 12.79 (s, 1H), 8.35−8.32 (dd, J = 7.0, 2.3 Hz, 1H), 7.62 (d, J = 8 Hz, 1H), 7.45−7.27 (m, 4H), 2.81 (s, 6H), 1.58 (s, 9H); ^{13}C NMR (75 MHz, $CDCl_3$) δ = 153.7, 150.3, 137.0, 136.1, 126.4, 125.3, 122.0, 119.3, 117.6, 114.1, 79.2, 45.9, 28.5; IR (neat) 3050 cm^{-1} (C−H, aromatic stretch), 2973 cm^{-1}, 2932 cm^{-1}, 2873 cm^{-1} (C−H stretch, alkane), 1709 cm^{-1} (N−H bend), 1638 cm^{-1} (C═O stretch, amide), 1135 cm^{-1} (C−O stretch); HRMS (ESI) m/z calcd for $C_{17}H_{22}N_2O_2$ $(M + H)^+$ 287.1754, found 287.1748.

*N^1,N^1-Dimethylnaphthalene-1,8-diamine (**7**).* To a 50 mL round-bottom flask containing 250 mg (0.873 mmol, 1 equiv) of **6**, backfilled with $N_{2(g)}$, was added 15 mL of dichloromethane. To the resulting mixture was added dropwise 2.67 mL (34.92 mmol, 40 equiv) of trifluoroacetic acid, and the reaction was allowed to stir for 12 h at room temperature. The crude product was diluted with 50 mL of H_2O, quenched with 37 mL of 1 M NaOH, and extracted three times with 10 mL of dichloromethane. The combined organic extracts were dried over $MgSO_4$, gravity-filtered through a funnel, and the solvent removed under reduced pressure. Purified compound could be acquired by flash chromatography (11% ethyl acetate in hexanes). The final product was obtained as a brown oil in a 90% yield (0.830 mmol, 154.5 mg): ^{1}H NMR (300 MHz, $CDCl_3$) δ = 7.54 (d, J = 8.2 1H), 7.34 (t, J = 7.6 Hz, 1H), 7.28 (t, J = 7.6 Hz, 1H), 7.18 (d, J = 7.6 Hz, 2H), 6.64 (dd, J = 7.4, 1.1, 1H), 6.18 (br s, 2H); ^{13}C NMR (75 MHz, $CDCl_3$) δ = 152.1, 145.5, 137.0, 126.6, 125.4, 125.4, 118.7, 117.0, 115.1, 109.7, 46.2; IR (neat) 3446 cm^{-1}, 3276 cm^{-1} (N−H stretch, primary amine), 3050 cm^{-1} (C−H, aromatic stretch), 2938 cm^{-1}, 2828 cm^{-1}, 2784 cm^{-1} (C−H stretch, alkane), 1590 cm^{-1} (N−H bend); HRMS (ESI) m/z calcd for $C_{12}H_{14}N_2$ $(M + H)^+$ 187.1230, found 186.1239.

*N-(2,3-Bis(diisopropylamino)cycloprop-2-en-1-ylidene)-8-(dimethylamino)naphthalen-1-aminium Chloride (Janus·HCl) (**9**).* To a solution of tetrachlorocyclopropene, **5** (0.025 mL, 0.2 mmol), which was prepared according to reported procedures, in dichloromethane (2 mL) was added freshly distilled diisopropylamine (0.11 mL, 0.8 mmol) dropwise under an inert nitrogen atmosphere. The reaction was stirred for 4 h at room temperature, after which **7** was added dropwise as a solution in dichloromethane (16 mg, 0.1 mmol), and the reaction was stirred for an additional 8 h. The crude product was purified by flash chromatography in (11% methanol in DCM) to afford **9** as an off-white solid in 90% yield (59 mg, 0.08 mmol); mp = 225−230 °C. Subsequent X-ray quality single crystals were grown from benzene and ethyl acetate (see below): ^{1}H NMR (300 MHz, $CDCl_3$) δ = 13.81 (s, 1H), 7.74−7.71 (m, 1H), 7.55−7.50 (m, 3H), 7.44−7.38 (m, 1H), 6.97 (d, J = 7.0 Hz,1H), 4.03−3.94 (m, 4H), 2.84 (s, 6H) 1.41 (d, J = 6.75 Hz, 24H) 2.75 (s, 6H), 1.14 (d, J = 6.8 Hz, 24H); ^{13}C NMR (75 MHz, $CDCl_3$) δ = 150.3, 138.2, 136.2, 126.9, 126.7, 125.3, 123.2, 119.9, 119.4, 118.9, 112.3, 110.0, 51.4, 46.4, 22.1; IR (neat) 3050 cm^{-1} (C−H, aromatic stretch), 2965 cm^{-1}, 2788 cm^{-1} (C−H stretch, alkane), 1709 cm^{-1} (N−H bend), 1524 cm^{-1} (C═C stretch, aromatic), 1489 cm^{-1} (C−N stretch); HRMS (ESI) m/z calcd for $C_{27}H_{41}N_4$ $(M + H)^+$ 421.3326, found 421.3331 (the HCl salt was not observed).

X-ray quality crystals were obtained as follows: **9** was dissolved in vial using slightly more than the minimal amount of benzene required for dissolution. The vial was then placed in a beaker filled 0.5 in. deep with ethyl acetate. The beaker was then capped with aluminum foil and placed in a 5 °C refrigerator, unperturbed for 72 h.

*N^1-(2,3-Bis(diisopropylamino)cycloprop-2-en-1-ylidene)-N^8,N^8-dimethylnaphthalene-1,8-diamine (Freebase of Janus) (**3**).* Synthesis of 1,8-bis(bis(diisopropylamino)cyclopropeniminenaphthalene, **3**: To a suspension of **6** (35 mg, 0.05 mmol) in toluene (2 mL) under an inert atmosphere was added dropwise dry potassium bis-(trimethylsilyl)amide (KHMDS, 0.5 M in toluene (0.5 mL, 0.25 mmol). The reaction was stirred for 2 h. The volatile components were removed under reduced pressure, and the product was extracted with hot hexane. The resulting product was isolated as yellow crystals in ca. 92% yield (25 mg, 0.04 mmol); mp = 94−95 °C: ^{1}H NMR (300 MHz, $CDCl_3$) δ = 7.37 (dd, J = 8.1, 1.1 Hz, 1H), 7.30−7.19 (m, 3H), 7.03−7.00 (m, 1H), 6.88 (dd, J = 7.6, 1.2 Hz, 1H), 3.51−3.38 (m, 4H), 2.75 (s, 6H), 1.14 (d, J = 6.8 Hz, 24H); ^{13}C NMR (75 MHz, $CDCl_3$) δ = 152.4, 137.7, 125.6, 124.7, 122.5, 120.7, 120.1, 112.8, 112.1, 49.0, 45.5, 22.1; IR (neat) 2965 cm^{-1}, 2925 cm^{-1} (C−H stretch, aromatic), 2818 cm^{-1}, 2765 cm^{-1} (C−H stretch, alkane), 1895 cm^{-1} (N−H bend), 1525 cm^{-1} (C═C stretch, aromatic), 1431 cm^{-1} (C−N stretch); HRMS (ESI) m/z calcd for $C_{27}H_{40}N_4$ (M^+) 420.3326, found 420.3326.

■ ASSOCIATED CONTENT

Supporting Information

The Supporting Information is available free of charge on the ACS Publications website at DOI: 10.1021/acs.joc.5b01743.

X-ray crystallographic data of compound **9** (CIF)

Coordinate and thermochemical data for all structures, QTAIM analysis, additional computed MOs for **3** and **9**,

DOI: 10.1021/acs.joc.5b01743
J. Org. Chem. 2016, 81, 6−13

NMR spectra for all reported compounds, including the ^{1}H NMR-based pK_a measurement (PDF)

AUTHOR INFORMATION

Corresponding Author

*E-mail: tdudding@brocku.ca.

Notes

The authors declare no competing financial interest.

ACKNOWLEDGMENTS

The authors would like to thank Alphora Research Inc. for HMRS analysis, Dr. Jeffrey Stuart for use of his fluorescence spectrophotometer, and Sharcnet for computing resources. Financial support was provided in part by NSERC. L.B. is grateful for a NSERC CGS scholarship.

REFERENCES

(1) Alder, R. W.; Bowman, P. S.; Steele, W. R. S.; Winterman, D. R. *Chem. Commun.* **1968**, *452*, 723−724.

(2) (a) Perrin, C. L.; Ohta, B. K. *J. Am. Chem. Soc.* **2001**, *123*, 6520−6526. (b) Hodgson, P.; Lloyd-Jones, G. C.; Murray, M.; Peakman, T. M.; Woodward, R. L. *Chem. - Eur. J.* **2000**, *6*, 4451−4460. (c) Howard, S. T. *J. Am. Chem. Soc.* **2000**, *122*, 8238−8244. (d) Raab, V.; Harms, K.; Sundermeyer, J.; Kovacević, B.; Maksić, Z. B. *J. Org. Chem.* **2003**, *68*, 8790−8797. (e) Llamas-Saiz, A. L.; Foces-Foces, C.; Elguero, J. *J. Mol. Struct.* **1994**, *328*, 297−323. (f) Raab, V.; Gauchenova, E.; Merkoulov, A.; Harms, K.; Sundermeyer, J.; Kovacevic, B.; Maksic, Z. B. *J. Am. Chem. Soc.* **2005**, *127*, 15738−15743.

(3) (a) Gerlt, J.; Gassman, P. *J. Am. Chem. Soc.* **1993**, *115*, 11552−11568. (b) Gerlt, J.; Gassman, P. *Biochemistry* **1993**, *32*, 11943−11952. (c) Frey, P.; Whitt, S.; Tobin, J. *Science* **1994**, *264*, 1927−1930. Guthrie, J. P. *Chem. Biol.* **1996**, *3*, 163−170. (d) Cox, C.; Wack, H.; Lectka, T. *Angew. Chem., Int. Ed.* **1999**, *38*, 798−800.

(4) Ozeryanskii, V. A.; Pozharskii, A. F.; Filarowski, A.; Borodkin, G. S. *Org. Lett.* **2013**, *15*, 2194−2197.

(5) (a) Szemik-Hojniak, A.; Rettig, W.; Deperasińska, I. *Chem. Phys. Lett.* **2001**, *343*, 404−412. (b) Szemik-Hojniak, A.; Balkowski, G.; Wurpel, G. W. H.; Herbich, J.; van der Waals, J. H.; Buma, W. J. *J. Phys. Chem. A* **2004**, *108*, 10623−10631. (c) Balkowski, G.; Szemik-Hojniak, A.; van Stokkum, I. H. M.; Zhang, H.; Buma, W. J. *J. Phys. Chem. A* **2005**, *109*, 3535−3541.

(6) (a) Scerba, M. T.; DeBlase, A. F.; Bloom, S.; Dudding, T.; Johnson, M. A.; Lectka, T. *J. Phys. Chem. A* **2012**, *116*, 3556−3560. (b) Scerba, M. T.; Leavitt, C. M.; Diener, M. E.; DeBlase, A. F.; Guasco, T. L.; Siegler, M. A.; Bair, N.; Johnson, M. A.; Lectka, T. *J. Org. Chem.* **2011**, *76*, 7975−7984.

(7) (a) Yoshida, Z.; Tawara, Y. *J. Am. Chem. Soc.* **1971**, *93*, 2573−2574. (b) Weiss, R.; Schloter, K. *Tetrahedron Lett.* **1975**, *16*, 3491−3494. (c) Weiss, R. *Tetrahedron Lett.* **1979**, *20*, 3295−3296. (d) Weiss, R.; Hertel, M. *J. Chem. Soc., Chem. Commun.* **1980**, 223−224.

(8) (a) Roberts, J. D.; Streitwieser, A., Jr.; Regan, C. I. *J. Am. Chem. Soc.* **1952**, *74*, 4579. (b) Breslow, R. *J. Am. Chem. Soc.* **1957**, *79*, 5318. (c) Breslow, R.; Groves, J. T. *J. Am. Chem. Soc.* **1970**, *92*, 984−987.

(9) Bandar, J. S.; Lambert, T. H. *Synthesis* **2013**, *45*, 2485−2498.

(10) (a) Bandar, J. S.; Lambert, T. H. *J. Am. Chem. Soc.* **2012**, *134*, 5552−5555. (b) Bandar, J. S.; Lambert, T. H. *J. Am. Chem. Soc.* **2013**, *135*, 11799−11802. (c) Wilde, M. M. D.; Gravel, M. *Angew. Chem., Int. Ed.* **2013**, *52*, 12651−12654. (d) Bandar, J. S.; Barthelme, A.; Mazori, A. Y.; Lambert, T. H. *Chem. Sci.* **2015**, *6*, 1537−1547. (e) Mirabdolbaghi, R.; Dudding, T. *Org. Lett.* **2015**, *17*, 1930−1933.

(11) (a) Mirabdolbaghi, R.; Dudding, T.; Stamatatos, T. *Org. Lett.* **2014**, *16*, 2790−2793. (b) Bandar, J. S.; Tanaset, A.; Lambert, T. H. *Chem. - Eur. J.* **2015**, *21*, 7365−7368.

(12) (a) Curnow, O. J.; MacFarlane, D. R.; Walst, K. J. *Chem. Commun.* **2011**, *47*, 10248−10250. (b) Curnow, O. J.; Holmes, M. T.; Ratten, L. C.; Walst, K. J.; Yunis, R. *RSC Adv.* **2012**, *2*, 10794−10797.

(13) Jiang, Y.; Freyer, J. L.; Cotanda, P.; Brucks, S. D.; Killops, K. L.; Bandar, J. S.; Torsitano, C.; Balsara, N. P.; Lambert, T. H.; Campos, L. M. *Nat. Commun.* **2015**, *6*, 5950.

(14) (a) Bruns, H.; Patil, M.; Carreras, J.; Vazquez, A.; Thiel, W.; Goddard, R.; Alcarazo, M. *Angew. Chem., Int. Ed.* **2010**, *49*, 3680−3683. (b) Kozma, Á.; Gopakumar, G.; Farès, C.; Thiel, W.; Alcarazo, M. *Chem. - Eur. J.* **2013**, *19*, 3542−3546.

(15) (a) Kovačević, B.; Maksić, Z. B.; Vianello, R. *J. Chem. Soc., Perkin Trans. 2* **2001**, 886−891. Gattin, Z.; Kovačević, B.; Maksić, Z. B. *Eur. J. Org. Chem.* **2005**, *15*, 3206−3213. (b) Margetić, D.; Ishikawa, T.; Kumamoto, T. *Eur. J. Org. Chem.* **2010**, *34*, 6563−6572. (c) Barić, D.; Dragičević, I.; Kovačević, B. *Tetrahedron* **2014**, *70*, 8571−8576.

(16) Belding, L.; Dudding, T. *Chem. - Eur. J.* **2014**, *20*, 1032−1037.

(17) (a) Llamas-Saiz, A. L.; Foces-Foces, C.; Elguero, J.; Molina, P.; Alajarin, M.; Vidal, A. *J. Chem. Soc., Perkin Trans. 2* **1991**, 2033−2040. (b) Cox, C.; Wack, H.; Lectka, T. *Angew. Chem., Int. Ed.* **1999**, *38*, 798−800. (c) Ozeryanskii, V. A.; Pozharskii, A. F.; Koroleva, M. G.; Shevchuk, D. A.; Kazheva, O. N.; Chekhlov, A. N.; Shilov, G. V.; Dyachenko, O. A. *Tetrahedron* **2005**, *61*, 4221−4232. (d) Kostyanovsky, R. G.; Pozharskii, A. F.; Nelyubina, Y. V.; Lyssenko, K. A.; Kadorkina, G. K.; Degtyarev, A. V.; Nabiev, O. G.; Chervin, I. I. *Mendeleev Commun.* **2008**, *18*, 86−87. (e) Mazaleyrat, J. P.; Wright, K. *Tetrahedron Lett.* **2008**, *49*, 4537−4541. (f) Brancatelli, G.; Drommi, D.; Feminò, G.; Saporita, M.; Bottari, G.; Faraone, F. *New J. Chem.* **2010**, *34*, 2853−2860. (g) Ozeryanskii, V. A.; Pozharskii, A. F.; Filarowski, A.; Borodkin, G. S. *Org. Lett.* **2013**, *15*, 2194−2197.

(18) Janus was the Roman god of beginnings and transitions, often depicted with two faces.

(19) Sauer, M.; Yeung, C.; Chong, J. H.; Patrick, B.; MacLachlan, M. J. *J. Org. Chem.* **2006**, *71*, 775−788.

(20) (a) Szemik-Hojniak, A.; Zwier, J. M.; Buma, W. J.; Bursi, R.; van der Waals, J. H. *J. Am. Chem. Soc.* **1998**, *120*, 4840−4844. (b) Pozharskii, A. F.; Ryabtsova, O. V.; Ozeryanskii, V. A.; Degtyarev, A. V.; Kazheva, O. N.; Alexandrov, G. G.; Dyachenko, O. A. *J. Org. Chem.* **2003**, *68*, 10109−10122. (c) Pozharskii, A. F.; Degtyarev, A. V.; Ryabtsova, O. V.; Ozeryanskii, V. A.; Kletskii, M. W.; Starikova, Z. A.; Sobczyk, L.; Filarowski, A. *J. Org. Chem.* **2007**, *72*, 3006−3019.

(21) (a) Raab, V.; Kipke, J.; Gschwind, R. M.; Sundermeyer, J. *Chem. - Eur. J.* **2002**, *8*, 1682−1693. (b) Raab, V.; Gauchenova, E.; Merkoulov, A.; Harms, K.; Sundermeyer, J.; Kovačević, B.; Maksic, Z. B. *J. Am. Chem. Soc.* **2005**, *127*, 15738−15743. (c) Belding, L.; Dudding, T. *Chem. - Eur. J.* **2014**, *20*, 1032−1037.

(22) (a) Weiss, R.; Brenner, T.; Hampel, F.; Wolski, A. *Angew. Chem.* **1995**, *107*, 481−483. (b) Weiss, R.; Brenner, T.; Hampel, F.; Wolski, A. *Angew. Chem., Int. Ed. Engl.* **1995**, *34*, 439−441. (c) Weiss, R.; Rechinger, M.; Hampel, F.; Wolski, A. *Angew. Chem., Int. Ed. Engl.* **1995**, *34*, 441−443.

(23) (a) Weiss, R.; Schloter, K. *Tetrahedron Lett.* **1975**, *16*, 3491−3494. (b) Azhar Hashmi, S. M.; Prasanna, S.; Radhakrishnan, T. P. *Synth. Met.* **1992**, *48*, 39−47.

(24) (a) Schleyer, P. v. R.; Maerker, C.; Dransfeld, A.; Jiao, H.; Hommes, N. J. R. v. E. *J. Am. Chem. Soc.* **1996**, *118*, 6317−6318. (b) Chen, Z. F.; Wannere, C. S.; Corminboeuf, C.; Puchta, R.; Schleyer, P. v. R. *Chem. Rev.* **2005**, *105*, 3842−3888. (c) Schleyer, P. v. R.; Jiao, H.; Hommes, N. J. R. v. E.; Malkin, V. G.; Malkina, O. L. *J. Am. Chem. Soc.* **1997**, *119*, 12669−12670. (d) von Ragué Schleyer, P.; Manoharan, M.; Wang, Z.-X.; Kiran, B.; Jiao, H.; Puchta, R.; van Eikema Hommes, N. J. R. *Org. Lett.* **2001**, *3*, 2465−2468. (e) Fallah-Bagher-Shaidaei, H.; Wannere, C. S.; Corminboeuf, C.; Puchta, R.; Schleyer, P. v. R. *Org. Lett.* **2006**, *8*, 863−866.

(25) (a) Szemik-Hojniak, A.; Zwier, J. M.; Buma, W. J.; Bursi, R.; van der Waals, J. H. *J. Am. Chem. Soc.* **1998**, *120*, 4840−4844. (b) Szemik-Hojniak, A.; Rettig, W.; Deperasińska, I. *Chem. Phys. Lett.* **2001**, *343*, 404−412.

(26) (a) Szemik-Hojniak, A.; Balkowski, G.; Wurpel, G. W. H.; Herbich, J.; van der Waals, J. H.; Buma, W. J. *J. Phys. Chem. A* **2004**, *108*, 10623−10631. (b) Balkowski, G.; Szemik-Hojniak, A.; van

DOI: 10.1021/acs.joc.5b01743
J. Org. Chem. 2016, 81, 6−13

Stokkum, I. H. M.; Zhang, H.; Buma, W. J. *J. Phys. Chem. A* **2005**, *109*, 3535−3541.

DOI: 10.1021/acs.joc.5b01743
J. Org. Chem. 2016, 81, 6−13